

Double-Negative Mechanical Metamaterials Displaying Simultaneous Negative Stiffness and Negative Poisson's Ratio Properties

HEWAGE, Trishan, ALDERSON, Kim, ALDERSON, Andrew
<<http://orcid.org/0000-0002-6281-2624>> and SCARPA, Fabrizio

Available from Sheffield Hallam University Research Archive (SHURA) at:

<http://shura.shu.ac.uk/13897/>

This document is the author deposited version. You are advised to consult the publisher's version if you wish to cite from it.

Published version

HEWAGE, Trishan, ALDERSON, Kim, ALDERSON, Andrew and SCARPA, Fabrizio (2016). Double-Negative Mechanical Metamaterials Displaying Simultaneous Negative Stiffness and Negative Poisson's Ratio Properties. *Advanced Materials*, 28 (46), 10323-10332.

Copyright and re-use policy

See <http://shura.shu.ac.uk/information.html>

Copyright WILEY-VCH Verlag GmbH & Co. KGaA, 69469 Weinheim, Germany, 2013.

Supporting Information

for *Adv. Mater.*, DOI: 10.1002/adma.((please add manuscript number))

Double-Negative Mechanical Metamaterials Displaying Simultaneous Negative Stiffness and Negative Poisson's Ratio Properties

Trishan A. M. Hewage, Kim L. Alderson, Andrew Alderson, and Fabrizio Scarpa*

Analytical model: Generalised arrangement of multiple spring types (semi-infinite assembly)

A semi-infinite array of interlocked hexagon sub-units is assumed, with each keyway having a spring associated with it (the case of no spring in any given keyway thus corresponding to a spring type having zero spring stiffness). Each sub-unit has two edges of length l_1 along the x direction, and four edges of length l_2 oriented at an angle of α to the x direction. The parameters a , b_1 and b_2 define gaps between adjacent units (Figure 1). The total number of springs in the system is N , and the number of different spring types (i.e. spring stiffnesses) is m . Let N_i^v and N_i^o be the number of springs having stiffness k_i located in vertical and oblique hexagonal key positions, respectively.

The total work done by the springs in the vertical positions due to an infinitesimal change in the interlock gap perpendicular to the adjoining hexagonal faces, b_i , to $b_i + db_i$ is given by

$$W^v = \sum_{i=1}^m N_i^v \left(\frac{1}{2} k_i (db_i)^2 \right) \quad (S1)$$

Similarly, the total work done by the springs in the oblique positions due to a change in b_2 to $b_2 + db_2$ is

$$W^o = \sum_{i=1}^m N_i^o \left(\frac{1}{2} k_i (db_2)^2 \right) \quad (S2)$$

The total work done by all the springs in the assembly is given by,

$$W = W^v + W^o \quad (S3)$$

From Figure 1

$$b_1 = 2a \cot \alpha \quad (S4)$$

$$b_2 = a \csc \alpha \quad (S5)$$

giving

$$\frac{db_1}{da} = 2 \cot \alpha \quad (S6)$$

$$\frac{db_2}{da} = \csc \alpha \quad (S7)$$

From Equation (S1)-(S3), (S6) and (S7) we get,

$$W = \left(\frac{1}{2} (da)^2 \right) \left(4 \cot^2 \alpha \sum_{i=1}^m N_i^v k_i + \csc^2 \alpha \sum_{i=1}^m N_i^o k_i \right) \quad (S8)$$

Now, the strain energy per unit volume for loading in the x-direction is given by,

$$U = \frac{1}{2} E_x (d\varepsilon_x)^2 = \frac{1}{2} E_x \left(\frac{dX_{RVE}}{X_{RVE}} \right)^2 = \frac{1}{2} E_x \left(\frac{1}{X_{RVE}} \frac{dX_{RVE}}{da} \right)^2 (da)^2 \quad (S9)$$

where E_x is the Young's modulus in the x direction, ε_x is the true strain applied to the assembly in the x direction, given by

$$\varepsilon_x = \ln \left(\frac{X_{RVE}}{X_{RVE0}} \right) \quad (S10)$$

and X_{RVE} and X_{RVE0} are the instantaneous and initial length of the representative volume element (RVE) in the x direction. X_{RVE} is given by

$$X_{RVE} = 2(l_1 + l_2 \cos \alpha + a) \quad (S11)$$

From Equation (S11):

$$\frac{dX_{RVE}}{da} = 2 \quad (S12)$$

From the principle of conservation of energy,

$$U = \frac{W}{V} \quad (S13)$$

where V is the volume of the assembly.

Since there are 6 keyways per RVE, there are $N/6$ RVEs in the semi-infinite assembly.

Considering unit thickness in the z -direction, the volume of the assembly is then

$$V = \frac{NX_{RVE}Y_{RVE}}{6} \quad (S14)$$

where Y_{RVE} is the instantaneous length of the RVE in the y direction given by

$$Y_{RVE} = 2(l_2 \sin \alpha + a \cot \alpha) \quad (S15)$$

The strain energy per unit volume for loading in the x-direction is then given by Equation (S9), (S13) and (S14):

$$U = \frac{1}{2} E_x \left(\frac{1}{X_{RVE}} \frac{dX_{RVE}}{da} \right)^2 (da)^2 = \frac{6W}{NX_{RVE}Y_{RVE}} \quad (S16)$$

and from Equation (S8), (S11), (S12), (S15) and (S16), we get

$$E_x = \frac{3}{2} \left(\frac{4 \cos^2 \alpha \sum_{i=1}^m n_i^v k_i + \sum_{i=1}^m n_i^o k_i}{\sin^2 \alpha} \right) \left(\frac{l_1 + l_2 \cos \alpha + a}{l_2 \sin \alpha + a \cot \alpha} \right) \quad (\text{S17})$$

where $n_i^v = N_i^v/N$ and $n_i^o = N_i^o/N$ are the number densities of the spring having stiffness k_i in the vertical and oblique locations, respectively.

Similarly, the Young's modulus in the y-direction can be shown to be

$$E_y = \frac{3}{2} \left(\frac{4 \cos^2 \alpha \sum_{i=1}^m n_i^v k_i + \sum_{i=1}^m n_i^o k_i}{\cos^2 \alpha} \right) \left(\frac{l_2 \sin \alpha + a \cot \alpha}{l_1 + l_2 \cos \alpha + a} \right) \quad (\text{S18})$$

Finite assembly stiffness: reconciling assembly and single-element stiffnesses

Recall that the instantaneous Young's modulus is given by the slope of the stress-strain curve in the most general case:

$$E_y = \frac{d\sigma_y}{d\varepsilon_y} = \frac{\left(\frac{dF_y}{XZ} \right)}{\left(\frac{dY}{Y} \right)} \quad (\text{S19})$$

where $d\sigma_y$, $d\varepsilon_y$, dF_y and dY are the increments in stress, strain, force and displacement in the y direction, and X, Y and Z are the dimensions of the test specimen. Rearranging Equation (S19) the stiffness, k_y , is given by:

$$k_y = \frac{dF_y}{dY} = \frac{E_y XZ}{Y} \quad (\text{S20})$$

The stiffness is dependent on the dimensions of the test specimen, and the X, Y and Z lengths of the finite assembly in the x, y and z directions, respectively are:

$$X = N_x X_{RVE}$$

$$Y = N_y Y_{RVE} \quad (S22)$$

$$Z = 1 \quad (S23)$$

where N_x , and N_y are the number of RVEs along the x and y direction, and unit thickness is assumed in the z direction of the assembly.

Substituting Equation (S11), (S15), (S18) and (S21)-(S23) into (S20):

$$k_y = \frac{3N_x}{2N_y} \left(\frac{4 \cos^2 \alpha \sum_{i=1}^m n_i^v k_i + \sum_{i=1}^m n_i^o k_i}{\cos^2 \alpha} \right) \quad (S24)$$

Equation (S24) relates the metamaterial (assembly) stiffness k_y to the single element stiffnesses k_i .

When $\alpha = 60^\circ$:

$$k_y = \frac{6N_x}{N_y} \left(\sum_{i=1}^m n_i^v k_i + \sum_{i=1}^m n_i^o k_i \right) \quad (S25)$$

Similarly, it can be shown that in the x direction we have

$$k_x = \frac{3N_y}{2N_x} \left(\frac{4 \cos^2 \alpha \sum_{i=1}^m n_i^v k_i + \sum_{i=1}^m n_i^o k_i}{\sin^2 \alpha} \right) \quad (S26)$$

Application to the ‘Control’ (positive spring) assembly case

For the 7-sub-unit assembly of 6 sub-units surrounding a central sub-unit we consider the number of RVEs along the x direction to be equal to one (since there are no sub-units connected to the outside of the ring of 6 sub-units). Hence $N_x = 1$. From Figure 4a (main text) the jaw-to-jaw separation of the mechanical testing machine corresponds to ~ 2.5 repeat units along the y direction of the assembly. Hence $N_y = 2.5$. The finite assembly therefore corresponds to $N_x N_y = 2.5$ repeat units. Each repeat unit contains 6 keyways, corresponding to a total of $N = 2.5 \times 6 = 15$ ‘springs’ (keyways) in the assembly, of which 8 and 4 positive stiffness springs (k_l) are located in oblique ($n_l^o = 8/15$) and vertical ($n_l^v = 4/15$) positions, respectively. The remaining keyways contain no springs (i.e. $m = 2$, $k_2 = 0$, $n_2^o = 2/15$ and $n_2^v = 1/15$).

In this case, Equation (S25) becomes:

$$k_y = \frac{6k_1}{2.5} \cdot \frac{12}{15} = 1.92k_1 \quad (\text{S27})$$

From the slope of the force-displacement curve in Figure 3a for the single spring test specimen, the stiffness of a single spring element is $k_l = 3.2 \text{ N mm}^{-1}$, giving a predicted value of $k_y = 6.1 \text{ N mm}^{-1}$ from Equation (S27). This is in excellent agreement with the average value of $k_y = 6.3 \pm 0.4 \text{ N mm}^{-1}$ from the slope of the force-displacement curve in three tests on the assembly. This is also demonstrated in Figure 4 where the predicted ‘control’ metamaterial force-displacement data assuming a straight line with slope given by $k_y = 6.1 \text{ N mm}^{-1}$ is shown for comparison with the measured data for the assembly.

Application to the PMI foam assembly case

Following a similar consideration of the actual finite assembly (Figure 4b), and assuming the stiffness of the PU foams is negligible in comparison to the PMI foams, we find in this case the following parameters:

$N_x = 1, N_y = 3, N = 18, n_1^o = 0, n_1^v = 1/9, m = 2, k_2 = 0, n_2^o = 2/3$ and $n_2^v = 2/9$.

In this case, Equation (S25) becomes:

$$k_y = \frac{2k_1}{9} \quad (\text{S28})$$

Since the PMI foam inserts in the assembly were of different dimensions to the individual PMI foam compression specimens it is necessary to determine the stiffness of the inserts from the measured stiffness of the compression samples. In region 1 of the compression specimen, $k_1 \sim 2889 \text{ N mm}^{-1}$ for the compression sample of dimensions 35 mm (rise direction) \times 25 mm \times 25 mm (Figure 3b). Using an equivalent expression to Equation (S20) the PMI foam Young's modulus in region 1 is then $E_s = (2889/0.025^2)/(1/35) = 162 \text{ N mm}^{-2}$ (= 0.162 GPa).

The assembly PMI foam insert dimensions are 5 mm (rise direction) \times 10mm \times 10mm. Hence, the region 1 stiffness of the foam insert in the assembly is $k_I = E_s \times 10^2/5 = 3236 \text{ N mm}^{-1}$, giving a metamaterial stiffness in region 1, calculated from Equation (S28), of $k_y = 719 \text{ N mm}^{-1}$. This is in reasonable agreement with the measured value, determined from the slope of the force-displacement data of the assembly, in region 1 of $k_y = 686 \text{ N mm}^{-1}$ (see comparison of the predicted force-displacement trend, shown by the dot-dashed line, with the actual data between initial 'settling in' of the sub-units at low strain and the onset of the NS response in region 2 of Figure 4).

The transition to negative stiffness (beginning of region 2) occurs after ~ 3 mm displacement of the 35 mm thick compression sample (Figure 3b). So for the combined 10 mm total thickness of the two PMI inserts in the assembly, we would expect negative stiffness to commence ~ 1 mm after engagement of the sub-units (i.e. following the initial settling in at low strain). This agrees well with the data for the assembly.

In region 2, the negative stiffness of the compression sample, taken from the slope of the force-displacement data in this region (Figure 3b), is $k_I = -443 \text{ N mm}^{-1}$. Hence the region 2 PMI foam Young's modulus is $E_s = (-443/0.025^2)/(1/32) = -23 \text{ N mm}^{-2}$ (= -0.023 GPa). From the equivalent expression to Equation (S20), the stiffness of the assembly PMI foam insert in region 2 is $k_I = E_s \times 10^2 / 4.5 = -511 \text{ N mm}^{-1}$, which using Equation (S28), corresponds to an assembly stiffness of $k_y = -114 \text{ N mm}^{-1}$. Again, this is in reasonable agreement with the actual value of $k_y = -160 \text{ N mm}^{-1}$ from the slope of the force-displacement curve of the assembly in region 2 (Figure 4).

Hence the experimentally measured stiffnesses of the individual inserts and assemblies for the control and PMI foam cases validate the analytical model expressions.

Supporting Information Figures

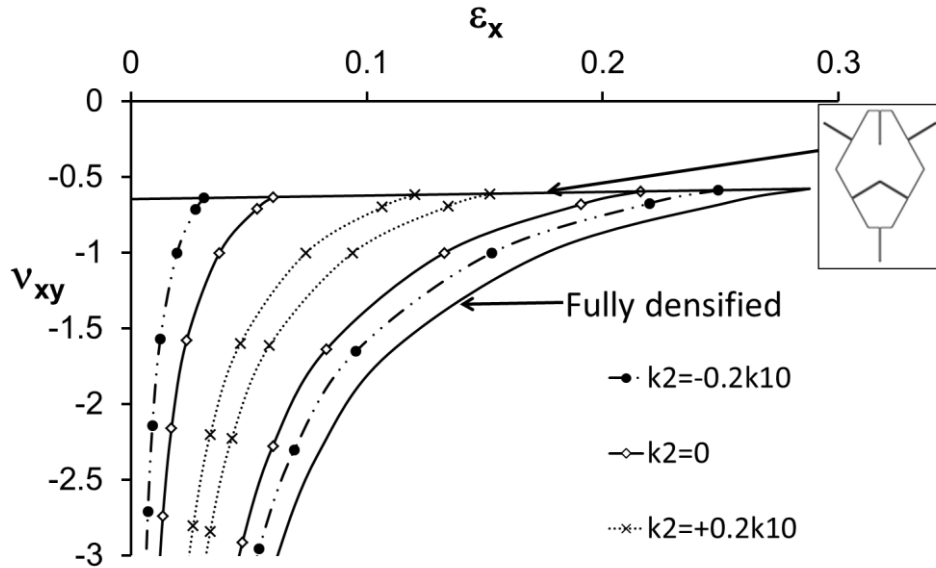


Figure S1. Dependency of mechanical metamaterial properties and strain on sub-unit length l_1 . Poisson's ratio (v_{xy}) as a function of global applied compressive strain (ϵ_x) for an assembly of sub-units of edge length $l_2 = 1$, $\alpha = 60^\circ$, infinitesimally narrow keyways having depths $\Delta_1 = \Delta_2 = 0.5l_2$, containing a buckled beam spring type (k_1 as in Figure 2a and 2c) occupying all vertical key locations ($n_1^v = 0.333$ and $n_1^o = 0$) and a constant stiffness spring type (k_2) occupying all oblique key locations ($n_2^v = 0$ and $n_2^o = 0.667$). Solid contours correspond to v_{xy} vs ϵ_x data when $E_x = 0$ (for $l_1 > 0.366l_2$) for $k_2 = -0.2k_{10}$, 0 and $0.2k_{10}$, and define enclosed regions of simultaneous negative Poisson's ratio and negative stiffness response. The boundaries are defined by inter-sub-unit geometrical constraints (fully expanded and fully densified structures) and intra-sub-unit constraints (when one female keyway intersects with another female keyway or another sub-unit edge).

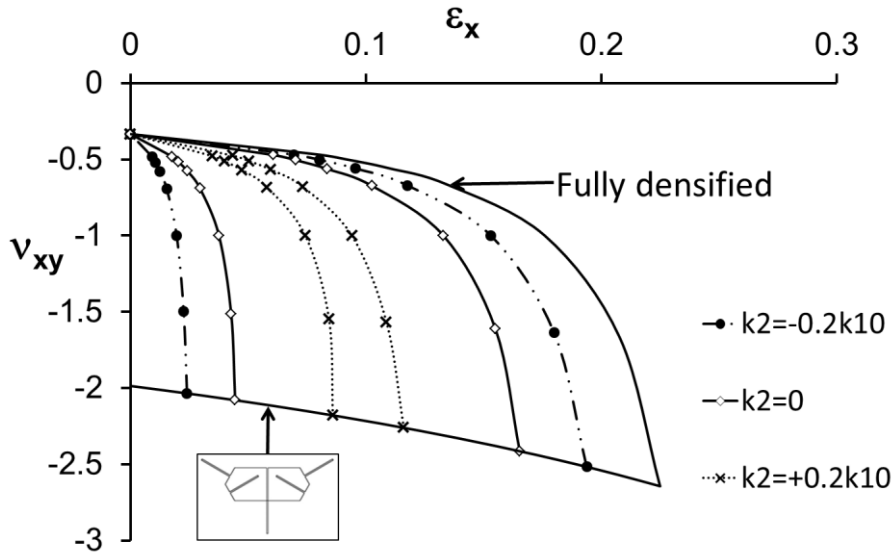


Figure S2. Dependency of mechanical metamaterial properties and strain on sub-unit length l_2 . Poisson's ratio (v_{xy}) as a function of global applied compressive strain (ϵ_x) for an assembly of sub-units of edge length $l_1 = 1$, $\alpha = 60^\circ$, infinitesimally narrow keyways having depths $\Delta_1 = \Delta_2 = 0.5l_1$, containing a buckled beam spring type (k_1 as in Figure 2a and 2c) occupying all vertical key locations ($n_1^v = 0.333$ and $n_1^o = 0$) and a constant stiffness spring type (k_2) occupying all oblique key locations ($n_2^v = 0$ and $n_2^o = 0.667$). Solid contours correspond to v_{xy} vs ϵ_x data when $E_x = 0$ (for $l_2 > 0.2886l_1$) for $k_2 = -0.2k_{10}$, 0 and $0.2k_{10}$, and define enclosed regions of simultaneous negative Poisson's ratio and negative stiffness response. The boundaries are defined by inter-sub-unit geometrical constraints (fully expanded and fully densified structures) and intra-sub-unit constraints (when one female keyway intersects with another female keyway or another sub-unit edge).

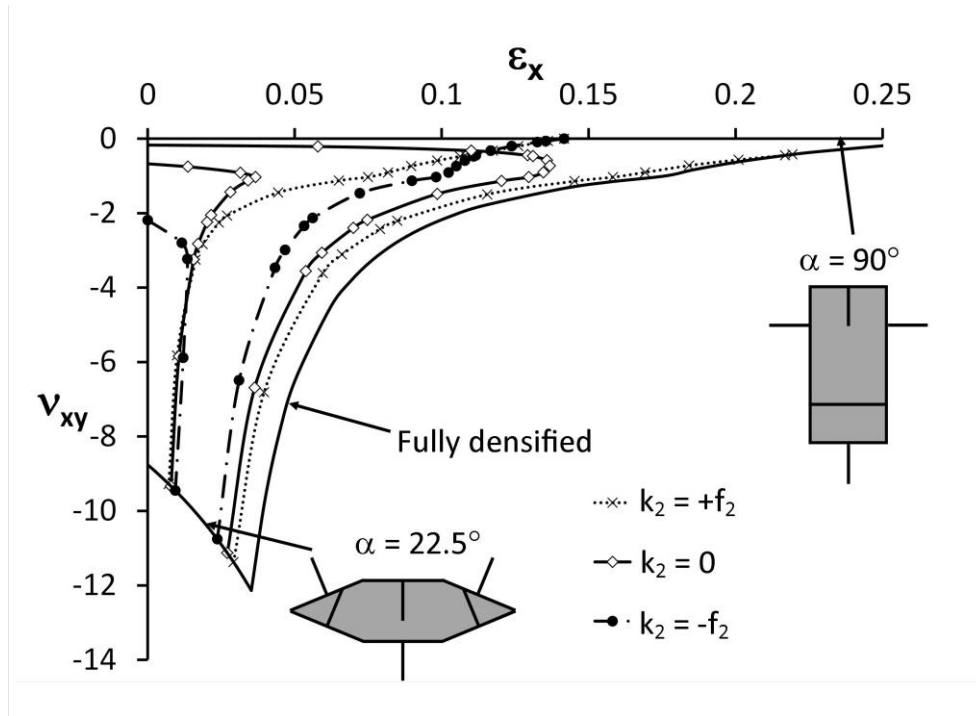


Figure S3. Dependency of mechanical metamaterial properties and strain on sub-unit angle. Poisson's ratio (v_{xy}) as a function of global applied compressive strain (ϵ_x) for an assembly of sub-units of edge lengths $l_1 = l_2$, infinitesimally narrow keyways having depths $\Delta_1 = \Delta_2 = 0.5l_1$, containing a buckled beam spring type (k_1 as in Figure 2a and 2c) occupying all vertical key locations ($n_1^v = 0.333$ and $n_1^o = 0$) and a second buckled beam spring type (k_2) occupying all oblique key locations ($n_2^v = 0$ and $n_2^o = 0.667$). Curves with symbols correspond to v_{xy} vs ϵ_x data when $E_x = 0$ (for $22.5 < \alpha < 90^\circ$) and define enclosed regions of simultaneous negative Poisson's ratio and negative stiffness response for $k_2 = -f_2, 0$ and $+f_2$, where f_2 is the stiffness function derived from the differential of the force-displacement function of spring 2 in Figure 2e. The boundaries are defined by inter-sub-unit geometrical constraints (fully expanded and fully densified structures) and intra-sub-unit constraints (when one female keyway intersects with another female keyway or another sub-unit edge).

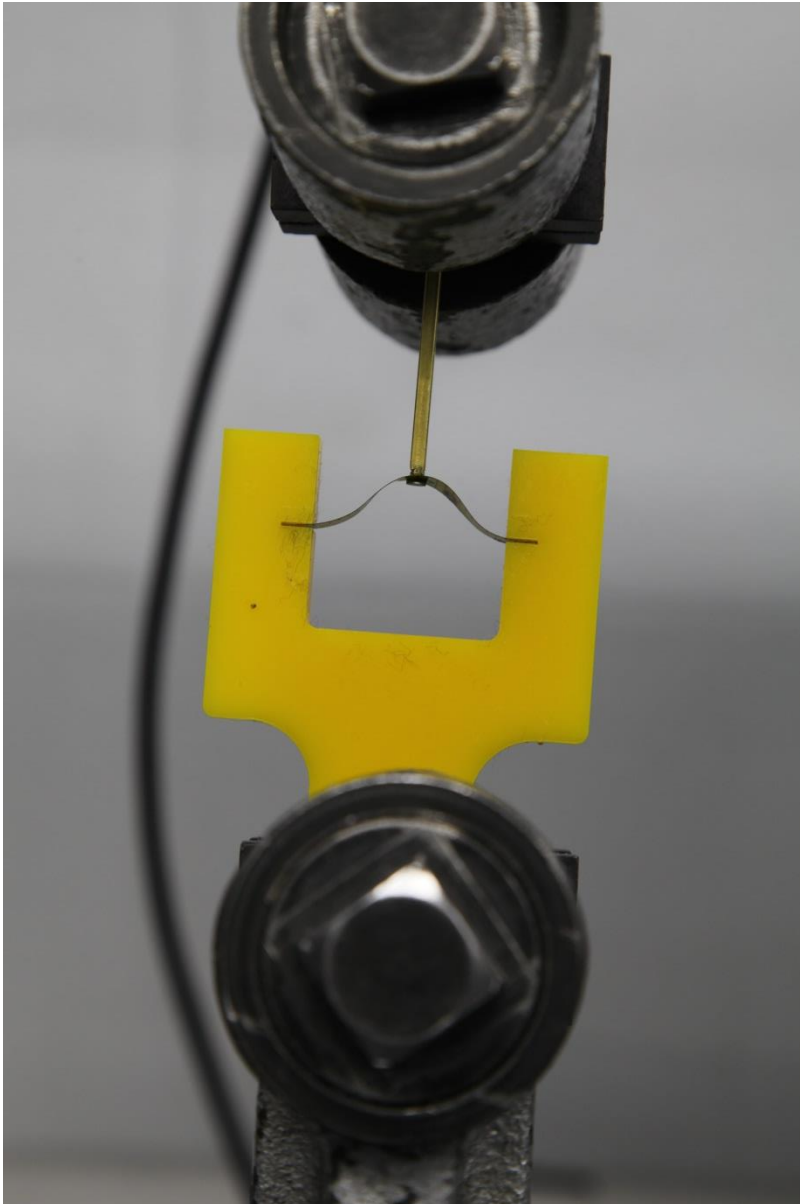


Figure S4. Single buckled beam and holder with rigid connector linking to moveable cross-head of mechanical testing machine.

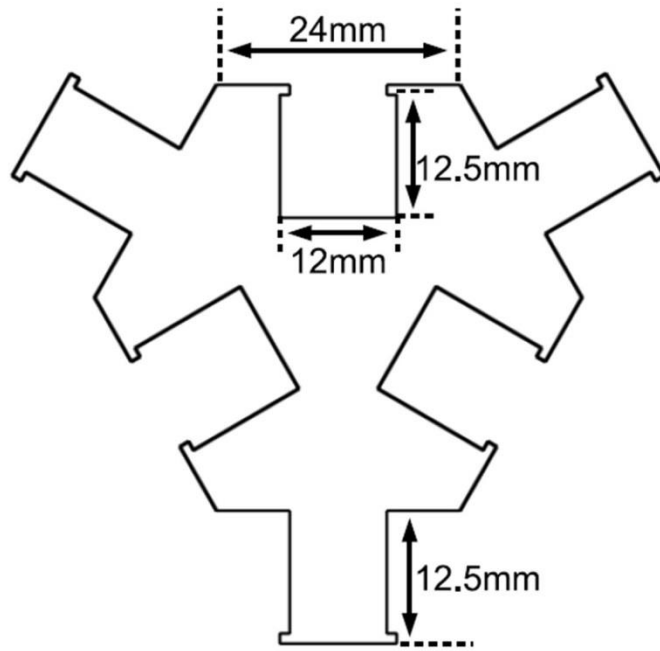


Figure S5. Design of sub-unit for PMI foam assembly.

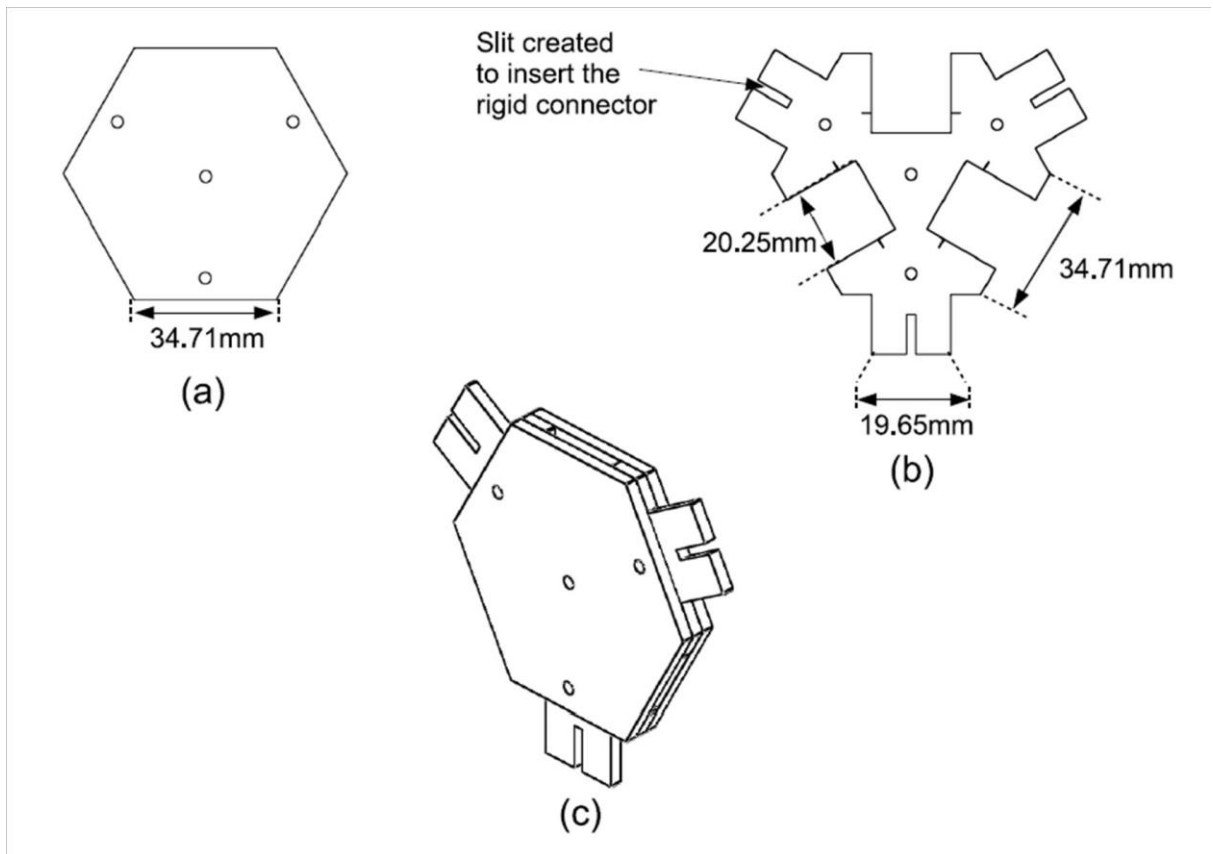


Figure S6. Design of sub-unit for Buckled beam assembly.

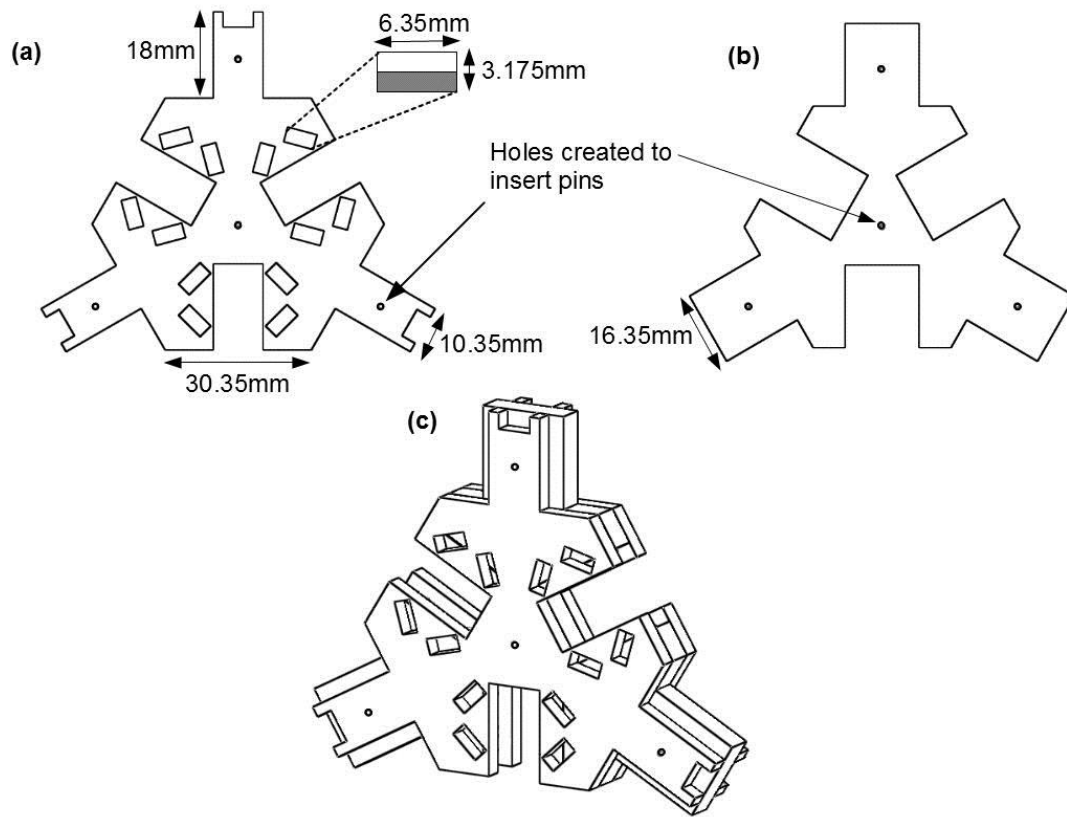


Figure S7. Design of sub-unit for Magnet assembly.

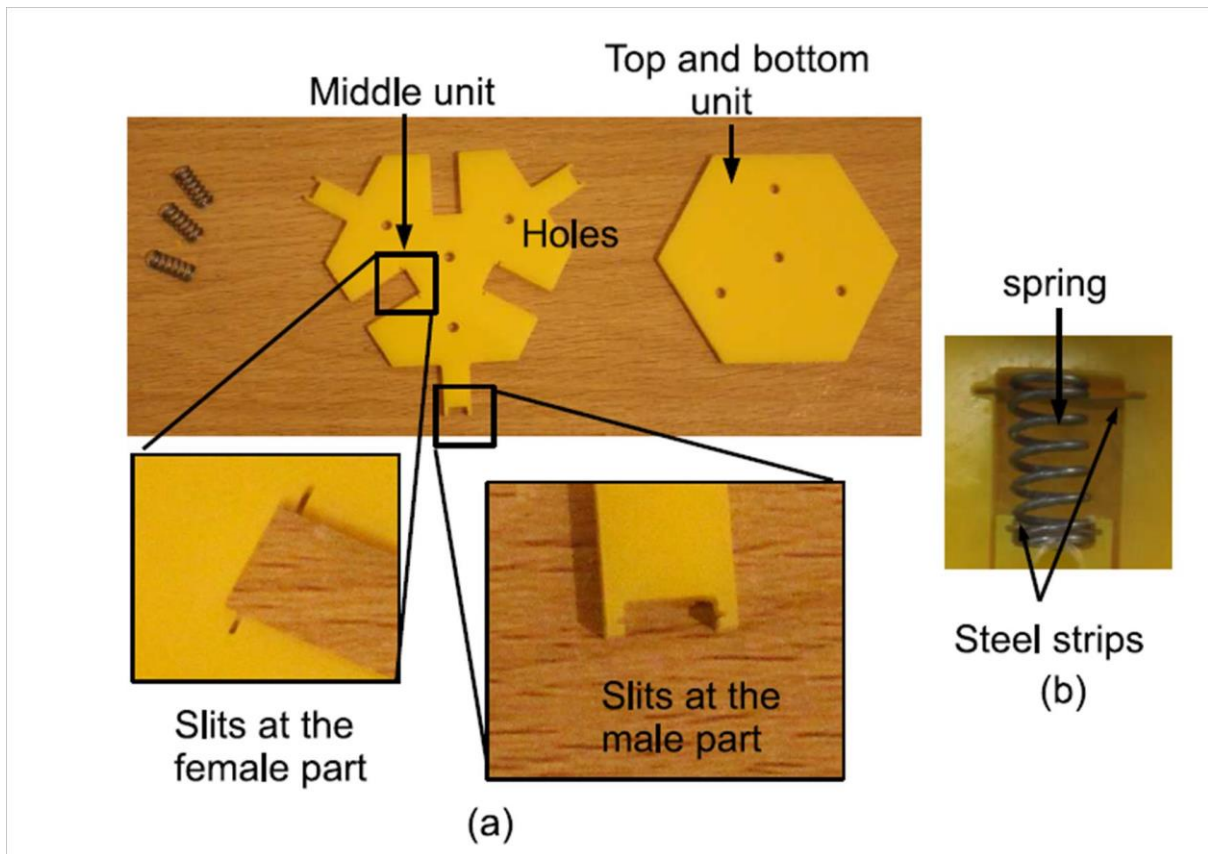


Figure S8. Components of sub-unit for 'Control' assembly.